

Visible Light Induced Photodegradation of Methylene Blue in Sodium Doped Bismuth Barium Ferrite Nanoparticle Synthesized by Sol-gel Method



Abdurrashid Haruna*, Ibrahim Abdulkadir, Suleiman Ola Idris

¹Department of Chemistry, Ahmadu Bello University, Zaria-Nigeria

*Correspondence to

Abdurrashid Haruna
Department of Chemistry,
Ahmadu Bello University,
Zaria, Nigeria
Email: abdurrashid.haruna@yahoo.com
Tel: +2348036507153

Published online December 29, 2018



Abstract

Perovskite-like BiFeO₃ nanoparticles doped with barium and sodium ions were synthesized via the citric acid route by the sol-gel method. The as-prepared Bi_{0.65}Na_{0.2}Ba_{0.15}FeO₃ nanopowders were divided into three equal portions and separately annealed at various annealing temperatures of 600, 700 and 800°C. The powders were characterized using X-ray diffraction (XRD) and crystallized with a rhombohedral R3c space group. Scanning electron microscopy was used to determine the morphology of the crystal and Fourier transform infrared spectroscopy was conducted at room temperature to determine the phase purity and the B-site formation in the perovskite structure. The UV-vis diffuse reflectance spectroscopy of all the materials was investigated, showing strong photoabsorption ($\lambda > 420$ nm). The doping effect of BiFeO₃ enhanced photocatalytic activity while it significantly reduced the energy bandgap to 2.05 eV (for BNBFO at 800°C) which showed strong visible light absorption. The photocatalytic activity of Bi_{0.65}Na_{0.2}Ba_{0.15}FeO₃ nanomaterials was tested by monitoring the degradation rate of methylene blue dye pollutant under visible light irradiation in aqueous solution. All powders showed photoactivity after 2 hours of visible light irradiation. The annealing temperature greatly affected the methylene blue degradation, showing the efficiencies of 57, 67 and 75 % for BNBFO at 600, 700 and 800°C, respectively. Kinetic studies were carried out and the rate constants of 6.70×10^{-3} , 8.90×10^{-3} and $1.05 \times 10^{-2} \text{ min}^{-1}$ were obtained for powders annealed at 600, 700 and 800°C, respectively. The photocatalytic mechanism of the degradation process was proposed in this study.

Keywords: Na doping, Sol-gel method, Methylene blue, Nanoparticles, Photocatalyst.

Received October 20 2018; Revised December 05, 2018; Accepted December 14, 2018

1. Introduction

Interestingly, a large number of perovskite nanoparticles have been discovered in the last few years. Perovskites are inorganic compounds with the general formula of ABO₃ (1). The A-site in the structure represents an alkaline-earth or a rare-earth (RE) element while the B-site is often a small element of the transition metal (2). The material was reported to have very fascinating multiferroic properties (3). The origin of these properties lies in the crystal structure of the material based on the synthesis procedure and route via which the material is prepared. A number of methods have been used for the preparation of BiFeO₃ (BFO) nanopowders. Scientists in various researches have prepared the material using widely accepted methods such as sol-gel (4), co-precipitation (5) and hydrothermal method (6). One method comes with a particular advantage over the other. The sol-gel method is simple and handy and it requires a temperature below 100°C for the preparation. Moreover, the process is cost-

effective and produces pure crystals with high yield.

Recently, the material has been shown to be very promising for practical applications because of its nontoxicity, low cost, and excellent chemical stability (7). The photocatalytic performance of these nanomaterials is drawing considerable attention especially in environmental remediation, sewage and wastewater treatments, air purification, industrial waste processes and destruction of toxic chemicals (8,9). The structure of BFO can be modified by doping at either of the sites to enhance the photocatalytic activity of the material.

The doping effect of BFO improved photoactivity of the catalyst under the visible light irradiation for the degradation of organic pollutants owing to its narrow band gap energy (2.0–2.75 eV). The study of the impact of a particular RE metal by doping into the structural, electronic and photocatalytic properties of the materials is, therefore, necessary (10). Soltani and Entezari (11) revealed that the photocatalytic activity of BFO can lead

to the production of hydrogen by water splitting in solar energy.

Other interesting applications of photocatalyst in environmental sanitation include photodegradation of volatile organic compounds for water treatment (12), germicidal and antimicrobial action (13), de-colorization of industrial dyes (8), nitrogen fixation in agriculture (14), and removal of several other air pollutants (9). It would be interesting to explore the possibilities of doping BFO with noble metals that will acts as photocatalyst for consideration in various potential applications. BFO was reported to have photocatalytic activity under visible light for the decomposition of methyl orange with band-gap energy values of 2.18–2.55 eV (15). Methylene blue (MB) is a cationic organic dye used in the textile industries. The removal of the dye from wastewater is necessary because it contaminates water, thereby making it toxic to aquatic lives. BFO and BFO related materials were used efficiently as photocatalyst in the removal of MB dye. The catalysts under visible light irradiation create valence band (VB) electrons and cause the electron to move to the conduction band (CB) leading to the generation of holes (16). The holes made are very active and can react directly with the organic contaminants on the surface of the catalyst. Huo et al (17) reported an energy band gap of 2.1 eV for BFO photocatalyst in MB photodegradation after 2 hours of visible light irradiation. BFO doped with Ca was reported to enhance the visible light response of the material for photocatalytic degradation bringing the degradation rate (C/C_0) of MB to 100% (18).

The photocatalytic activity, magnetic ordering, and doping effects of BFO material with noble metals (Na^+ , K^+ , Ca^{2+} , Sr^{2+} , Ba^{2+}) using both univalent and divalent metal ions were investigated (4,19,20). Therefore, the photocatalytic activities of the remaining BFO-doped semiconducting materials are needed to be explored at different concentrations of dopants until a suitable band gap energy is determined effective for photodegradation of pollutants under visible light irradiation.

In this research, pure perovskite-like $\text{Bi}_{0.65}\text{Na}_{0.2}\text{Ba}_{0.15}\text{FeO}_3$ nanoparticles with controlled size were prepared using the sol-gel method in the presence of sodium dodecyl sulfate (SDS) as a surfactant. The effect of annealing temperature on doping the material was investigated. The photocatalytic activities of the powders were determined against a methylene blue pollutant for degradation studies under visible light irradiation. The degradation rate of the dye was determined and the energy bandgap was calculated. Kinetic data were generated and the mechanism of the photodegradation process was proposed and discussed.

2. Materials and Methods

2.1. Materials

The chemicals used in this study were as follows: $\text{Bi}(\text{NO}_3)_3 \cdot 5\text{H}_2\text{O}$ (purity>99%), $\text{Ba}(\text{NO}_3)_2$ (purity>99%),

NaNO_3 (purity>99.0%), NaOH (98%), $\text{Fe}(\text{NO}_3)_3 \cdot 9\text{H}_2\text{O}$ (purity>98.5%), HCl (37%), SDS (average M.W. = 288.38), ($\text{C}_6\text{H}_8\text{O}_7 \cdot \text{H}_2\text{O}$; citric acid), ethylene glycol (purity>99%), and NH_4OH (30% NH_3). All chemicals were purchased with an analytical grade from Sigma-Aldrich and used without further purification. Distilled water was used throughout this work.

2.2. Synthesis Method of $\text{Bi}_{0.65}\text{Na}_{0.2}\text{Ba}_{0.15}\text{FeO}_3$ Nanoparticles

$\text{Bi}_{0.65}\text{Na}_{0.2}\text{Ba}_{0.15}\text{FeO}_3$ nanopowders were synthesized using the sol-gel method via the citric acid route in the presence of SDS. The nitrate precursors were calculated in stoichiometric amounts by taking 6.30 g of $\text{Bi}(\text{NO}_3)_3 \cdot 5\text{H}_2\text{O}$ and 0.78 g of $\text{Ba}(\text{NO}_3)_2$ to form an aqueous solution at room temperature. Then, 8.08 g of $\text{Fe}(\text{NO}_3)_3 \cdot 9\text{H}_2\text{O}$ and 0.34 g of NaNO_3 were added to the mixture and the whole solution was made up to 100 mL with distilled water until a homogeneous solution was formed. The solution in a beaker was then placed on a magnetic stirrer set at 90°C. The citric acid solution ($4.0 \times 10^{-1}\text{M}$) was added in dropwise with continuous heating and stirring process for about 40 minutes. Then, 10 mL of ethylene glycol was added as structure-directing and polymerization agent with continuous heating and stirring followed by the addition of 5 g of SDS (0.35M). The pH of the solution was maintained at 8 following the addition of a few drops of solution (30% NH_3). After about 1 hour, a dark yellow solution was formed which is then dried in an oven to give gel. The gel obtained was pre-calcined to obtain pure-phase powders. The obtained fine powders were separately annealed at temperatures of 600, 700 and 800°C for 4 hours. The sol-gel method was previously used to study BFO and BFO related nanoparticles (4,21).

2.3. Characterization

X-ray diffraction (XRD) analysis of the powders was conducted using the Rigaku Ultima IV X-ray diffractometer equipped with Cu K α radiation ($\lambda = 1.5406 \text{ \AA}$) at a scan rate of 10°/min. The accelerating voltage and the applied currents were 40 kV and 35 mA, respectively. Field emission scanning electron microscopy (SEM, JEOL/EO Version 1.0 JSM-6610) was used to study the morphology of the samples at an accelerating voltage of 40 kV and 40 mA having 3°/min speed. A 100 PerkinElmer FTIR spectrometer was used to collect the spectra of all the powdered samples. The Uv-visible absorption spectrum of the samples was determined using a Shimadzu 3101 spectrophotometer between 200–800 nm.

2.4. Studies of the Photocatalytic Activity

The photocatalytic activity of perovskite-like $\text{Bi}_{0.65}\text{Na}_{0.2}\text{Ba}_{0.15}\text{FeO}_3$ nanomaterials was investigated by the photodegradation studies of MB dye in aqueous solution under the visible light irradiation. To do so, 15 mg of the catalyst was used throughout the degradation studies. The dye solution (10 mg/L) was prepared by dissolving

10 mg of the dye in 1000 mL of distilled water at room temperature. The wavelength of maximum absorbance of the dye was scanned and recorded at 664 nm. A photoreactor was used throughout the photocatalytic studies with a magnetic stirrer set at 50 rpm using a 250 W Xe lamp ($\lambda > 400$ nm) (Osram, Germany). In the first experiment, 100 mL of the dye solution was used without catalyst under the dark condition at 20-minute intervals for 2 hours until adsorption equilibrium was reached. No activity was recorded for the blank dye solution in the absence of light and catalyst. The procedure was repeated with separate portions of the catalysts under visible light irradiation adjusting the pH of the solution to 7. 10 mL of the solution was pipetted each time after 20 minutes to monitor the absorbance using the Shimadzu UV-vis spectrophotometer. The degradation rate (C/C_0) of all samples was calculated and determined.

3. Results and Discussion

3.1 XRD Results of the $\text{Bi}_{0.65}\text{Na}_{0.2}\text{Ba}_{0.15}\text{FeO}_3$ Nanoparticles

A fine brown powder of BNBFO was obtained with high yield. The XRD pattern of the nanoparticles displayed high crystallinity as shown in Fig. 1. The diffractograms after matching were shown to be made up of single-phase crystals with a distorted rhombohedral structure belonging to R3c space group. The absence of impurity peaks is an indication that all ions have been incorporated into the perovskite structure. All the samples showed crystallinity, and powders annealed at 600°C and 700°C

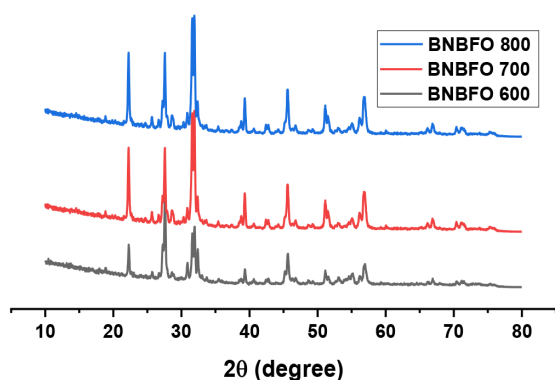


Fig. 1. XRD Results of BNBFO Nanoparticles Annealed at 600, 700 and 800°C.

displayed prominent perovskite peaks with a gradual increase in the peak intensities. The increase in peaks could be as a result of doping the ions into the structure of BFO nanoparticles. No significant change was observed in the peak intensities of the powdered nanoparticles except for gradual peak broadening of BNBFO at 800°C, indicating high crystallinity of the material. The average crystallite size of the powders was estimated using the Debye-Scherrer equation (1) as the annealing temperature was increased, which was found to be 29.68 ± 2 nm for BNBFO at 800°C. The results obtained are in good agreement with the results of other previously reported studies (4, 21).

$$D = K\lambda/\beta\cos\theta \quad (1)$$

Where K is the Scherrer constant, λ is the wavelength of radiation, θ is the Bragg angle, β is the full width at half maximum and D is the average crystallite size of the material.

3.2. SEM Results of the $\text{Bi}_{0.65}\text{Na}_{0.2}\text{Ba}_{0.15}\text{FeO}_3$ Nanoparticles

The SEM results of BNBFO nanoparticles annealed at 600–800°C are shown in Fig. 2. The results show the formation of polycrystalline nanoparticles. The powder annealed at 600°C (Fig. 2a) showed clustering of the particles indicating that even after doping, the structure of the material is maintained and no second phase was observed. At a temperature of 700°C, an increase was observed in the shape and size of the particles as shown

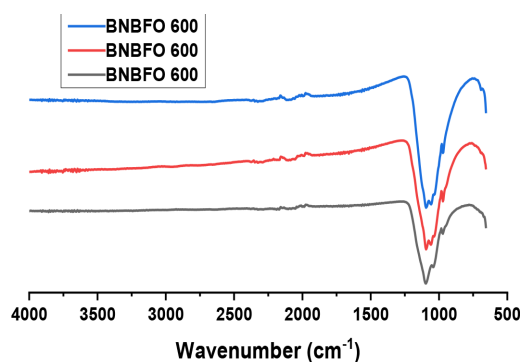


Fig. 3. FTIR Results of BNBFO Nanoparticles Annealed at 600, 700 and 800°C

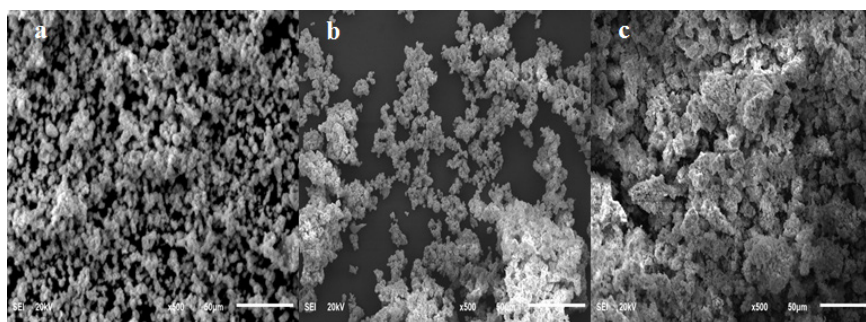


Fig. 2. SEM image of BNBFO Nanoparticles Annealed at 600, 700 and 800°C

in Fig. 2b. Fig. 2c shows agglomeration of the particles thereby affecting the morphology of the crystals for powder at 800°C. This is due to the increase in annealing temperature leading to an increase in the crystallinity of the material and hence increase in the particle size (20 to 80 nm). This result agrees very well with the presented XRD results.

3.3. FTIR Results of $\text{Bi}_{0.65}\text{Na}_{0.2}\text{Ba}_{0.15}\text{FeO}_3$ Nanoparticles

The FTIR results of $\text{Bi}_{0.65}\text{Na}_{0.2}\text{Ba}_{0.15}\text{FeO}_3$ nanopowders (600–800) were determined at room temperature for all the samples. Fig. 3 shows the spectra of the powdered nanoparticles. Stretching and bending vibrations for the formation of the perovskite structure were found to be in good agreement with the results presented for XRD. At around 850–1350 cm^{-1} , there is a broad absorbance peak which is assigned to the powdered crystals as a result of adsorbed water molecule onto the surface of the material (4). A decrease in the peak intensity suggests that more of the oxides have been properly incorporated into the perovskite structure due to the effect of doping the material. Stretching and bending vibrations at around 600 cm^{-1} is assigned to the metal-oxygen bonds for Fe–O and O–Fe–O in the perovskite structure (22).

3.4. UV-Vis DRS Spectrum of $\text{Bi}_{0.65}\text{Na}_{0.2}\text{Ba}_{0.15}\text{FeO}_3$ Nanoparticles

The optical absorption of all samples was measured using the Uv-Vis DRS spectrum as shown in Fig. 4. The materials showed strong photoabsorption within the visible light region (200–800 nm) of the electromagnetic spectrum and the powder annealed at 800°C had the highest wavelength of absorption. The photoabsorption of the powder may be as a result of appropriate incorporation of the sodium ion into the perovskite structure. The band gap energy of the semiconducting material with the highest optical absorptivity was determined. The inset in Fig. 4 shows how the band gap energy was extrapolated from Tauc's plot using equation (2) (23).

$$\alpha h\nu = C (h\nu - E_g)^n \quad (2)$$

Where $h\nu$ is the photon energy, α is the optical absorptivity coefficient, C is a constant known as the effective mass parameter, n is 1/2 for a direct transition, and E_g is the energy band gap (24). These materials may show a potential application in wastewater treatments with an extrapolated bandgap energy of 2.05 eV which is in agreements with the previous findings of other researchers having energy band gap values of 2.0 eV, 2.3 eV, and 2.1 eV (25).

3.5. The Photocatalytic Performance of BNBFO

The photocatalytic performance of all the powdered samples were investigated by the degradation studies of the model dye, MB pollutants, under visible light irradiation ($\lambda > 420$ nm) at 20-minute intervals for 2 hours. In the absence of catalyst throughout the degradation

process, the dye was found to be stable having no or little degradation rate (C/C_0), approximately 3%. As shown in Fig. 5, the degradation effect was so good for powders annealed at 600 and 700°C, and best at 800°C. Equation 3 is used to calculate the degradation efficiency of the dye, where C_0 and C_t are the initial and final concentrations of the dye before and after degradation process, respectively.

$$\frac{C_t - C_0}{C_0} \times 100 \quad (3)$$

The degradation efficiencies of BNBFO for MB removal were found to be 57, 67 and 75 % for powders at 600, 700, and 800°C, respectively. All powders exhibited an excellent visible light response, attributed to the doping with Na, which in-turn led to an increase in the photocatalytic properties of the powdered nanoparticles. Table 1 shows the comparison of the degradation rate of methylene blue with BNBFO and some other catalyst.

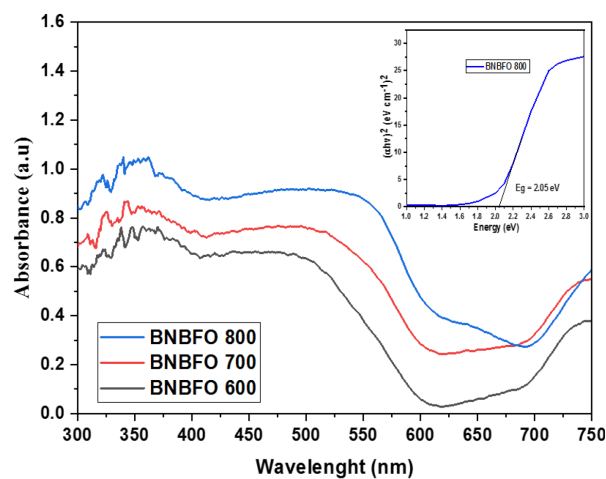


Fig. 4. DRS results of BNBFO Nanoparticles Annealed at 600, 700 and 800°C.

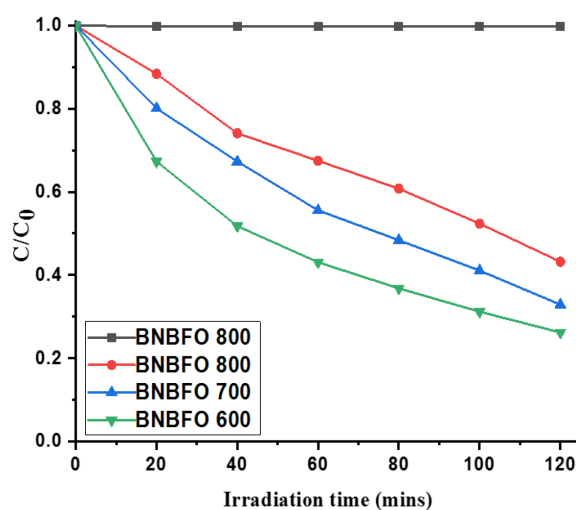


Fig. 5. Photocatalytic results of BNBFO Nanoparticles Annealed at 600, 700 and 800°C.

Table 1. Methylene Blue Removal with Different Catalyst

Catalyst	Method of Synthesis	Organic Dye	Initial Concentration of the Dye (mg/L)	Time (min)	Degradation (%)	Reference
BNBFO	Sol-gel method	Methylene blue	10.00	120	75	This study
	Solvothermal synthesis	Methylene blue	3.20	50	96	(26)
BFO	Solvothermal synthesis		10.00	240	86	(17)
	Ultrasound		1.50	90	100	(27)
TiO ₂	Hummer's method	Methylene blue	10.00	100	52	(28)
	-	Methylene blue	20.00	60	90	(29)
BFO-Dy	Sol-gel method	Methylene blue	1.00	240	92	(30)
BFO-Gd	Sol-gel method	Methylene blue	1.00	240	94	(31)
BFO-Sm	Sol-gel method	Methyl orange	5.00	120	65	(32)

Table 2. The Observed Rate Constant for the Photodegradation of MB Dye with the Photocatalyst

System	K _{obs} /min ⁻¹	R ²
BNBFO 600	6.70 x 10 ⁻³	0.9913
BNBFO 700	8.90 x 10 ⁻³	0.9966
BNBFO 800	1.05 x 10 ⁻²	0.9680

Fig. 6. MB Photodegradation and the First-order Kinetics.

The photocatalytic reaction for the degradation of MB follows the first-order kinetics as shown in Fig. 6. The rate constants for MB degradation based on the pseudo-first-order kinetics was determined quantitatively as shown in Table 2 using the equation.

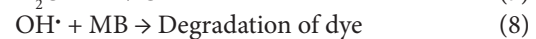
$$\ln(C_t/C_0) = k_{\text{obs}} t \quad (4)$$

Where k_{obs} is the observed rate constant, C_0 and C are the initial and final concentrations at time t (minutes), respectively for the dye (33). The rate of the reaction was found to increase with increasing annealing temperature. The rate of the degradation process with the catalyst increases with increasing the annealing temperature resulting in an increase in the rate constants of the pseudo-first-order kinetics. The rate constants for the materials, where the value of k was highest for BNBFO annealed at 800°C, may also be due to the doping into the perovskite structure leading to improved photocatalytic activity of the BNBFO nanoparticles.

3.6. Mechanism of MB Degradation

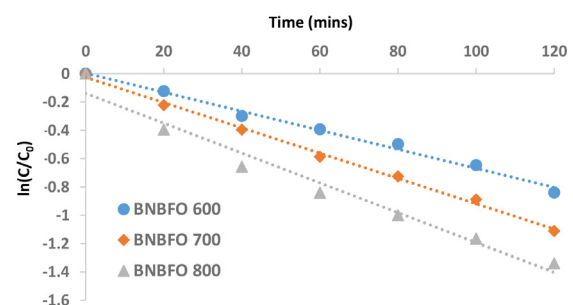
The following equations (5-8) show the photocatalytic reaction involved in the generation of electron-hole pairs. In the mechanistic pathway, the electron generated in the conduction band of the catalyst is trapped by peroxide causing the production of radical species. The holes abstract electrons from absorbed dye or react with H₂O to form hydroxyl radicals. The electrons then reduce the absorbed molecular oxygen to yield superoxide anion radicals which can further disproportionate to form OH radicals via chain reactions. Both kinds of radicals can initiate redox reactions with organic molecules

absorbed on the surface of the photocatalyst which leads to the destruction of the dye. The radicals generated are responsible for the photodegradation of methylene blue dye.



4. Conclusion

Perovskite-like Bi_{0.65}Na_{0.2}Ba_{0.15}FeO₃ photocatalyst was prepared by the sol-gel method. The obtained single-phase powder had a distorted rhombohedral structure belonging to R3c space group. The material under visible light showed improved degradation of MB pollutants. The degradation rate of MB dye was evaluated and determined to be 57, 67 and 75 for powders annealed at 600, 700 and 800°C, respectively, after 2 hours of visible light irradiation. The annealing temperature affected the synthesis of Bi_{0.65}Na_{0.2}Ba_{0.15}FeO₃, which influenced the degradation of the dye. The energy bandgap for the powder with the highest visible light photoactivity (BNBFO at 800°C) was estimated to be 2.05 eV which shows that the material may have some promising applications in environmental remediation and wastewater treatment.

**Fig. 6.** MB Photodegradation and the First-order Kinetics.

Conflict of Interest Disclosures

The authors have no conflicts of interest to declare.

References

- Woodward PM. Octahedral tilting in perovskites. II. structure stabilizing forces. *Acta Crystallogr B*. 1997;53(1):44-66. doi: 10.1107/s0108768196012050.
- Yang Y, Sun Y, Jiang Y. Structure and photocatalytic property of perovskite and perovskite-related compounds. *Mater Chem Phys*-3. 2006;96(2):234-9. doi: 10.1016/j.matchemphys.2005.07.007.
- Tanaka H, Misono M. Advances in designing perovskite catalysts. *Curr Opin Solid State Mater Sci*. 2001;5(5):381-7. doi: 10.1016/S1359-0286(01)00035-3.
- Haruna A, Abdulkadir I, Idris SO. Synthesis, characterization and photocatalytic properties of Bi_{0.85}-XMXBa_{0.15}FeO₃ (M = Na and K, X = 0, 0.1) perovskite-like nanoparticles using the sol-gel method. *J King Saud Univ Sci*. 2019. doi: 10.1016/j.jksus.2019.05.005.
- Liu Z, Qi Y, Lu C. High efficient ultraviolet photocatalytic activity of BiFeO₃ nanoparticles synthesized by a chemical coprecipitation process. *J Mater Sci Mater Electron*. 2010;21(4):380-4. doi: 10.1007/s10854-009-9928-x.
- Wang Y, Xu G, Ren Z, Wei X, Weng W, Du P, et al. Mineralizer-Assisted Hydrothermal Synthesis and Characterization of BiFeO₃ Nanoparticles. *J Am Ceram Soc*. 2007;90(8):2615-7. doi: 10.1111/j.1551-2916.2007.01735.x.
- Grinberg I, West DV, Torres M, Gou G, Stein DM, Wu L, et al. Perovskite oxides for visible-light-absorbing ferroelectric and photovoltaic materials. *Nature*. 2013;503(7477):509-12. doi: 10.1038/nature12622.
- Ahmed S, Rasul MG, Martens WN, Brown R, Hashib MA. Advances in heterogeneous photocatalytic degradation of phenols and dyes in wastewater: a review. *Water Air Soil Pollut*. 2011;215(1-4):3-29. doi: 10.1007/s11270-010-0456-3.
- Guo C, Wu X, Yan M, Dong Q, Yin S, Sato T, et al. The visible-light driven photocatalytic destruction of NO_x using mesoporous TiO₂ spheres synthesized via a "water-controlled release process". *Nanoscale*. 2013;5(17):8184-91. doi: 10.1039/C3NR02352D.
- Grabowska E. Selected perovskite oxides: characterization, preparation and photocatalytic properties--A review. *Appl Catal B Environ*. 2016;186:97-126. doi: 10.1016/j.apcatb.2015.12.035.
- Soltani T, Entezari MH. Solar-Fenton catalytic degradation of phenolic compounds by impure bismuth ferrite nanoparticles synthesized via ultrasound. *Chem Eng J*. 2014;251:207-16. doi: 10.1016/j.cej.2014.04.021.
- Tan YN, Wong CL, Mohamed AR. An Overview on the Photocatalytic Activity of Nano-Doped-TiO₂ in the Degradation of Organic Pollutants. *ISRN Mater Sci*. 2011;2011:261219. doi: 10.5402/2011/261219.
- Pelaez M, Nolan NT, Pillai SC, Seery MK, Falaras P, Kontos AG, et al. A review on the visible light active titanium dioxide photocatalysts for environmental applications. *Appl Catal B Environ*. 2012;125:331-49. doi: 10.1016/j.apcatb.2012.05.036.
- Bickley RI, Vishwanathan V. Photocatalytically induced fixation of molecular nitrogen by near UV radiation. *Nature*. 1979;280(5720):306-8. doi: 10.1038/280306a0.
- Gao F, Chen XY, Yin KB, Dong S, Ren ZF, Yuan F, et al. Visible-light photocatalytic properties of weak magnetic BiFeO₃ nanoparticles. *Adv Mater*. 2007;19(19):2889-92. doi: 10.1002/adma.200602377.
- Samarghandi MR, Rahmani AR, Samadi MT, Kiamanesh M, Azarian G. Degradation of Pentachlorophenol in Aqueous Solution by the UV/ZrO₂/H₂O₂ Photocatalytic Process. *Avicenna J Environ Health Eng*. 2015;2(2):e4761. doi: 10.17795/ajehe-4761.
- Huo Y, Jin Y, Zhang Y. Citric acid assisted solvothermal synthesis of BiFeO₃ microspheres with high visible-light photocatalytic activity. *J Mol Catal A Chem*. 2010;331(1-2):15-20. doi: 10.1016/j.molcata.2010.08.009.
- Ramadan W, Shaikh PA, Ebrahim S, Ramadan A, Hannover B, Jouen S, et al. Highly efficient photocatalysis by BiFeO₃/α(γ)-Fe₂O₃ ferromagnetic nano p/n junctions formed by dopant-induced phase separation. *J Nanopart Res*. 2013;15(8):1848. doi: 10.1007/s11051-013-1848-2.
- Soltani T, Lee BK. Novel and facile synthesis of Ba-doped BiFeO₃ nanoparticles and enhancement of their magnetic and photocatalytic activities for complete degradation of benzene in aqueous solution. *J Hazard Mater*. 2016;316:122-33. doi: 10.1016/j.jhazmat.2016.03.052.
- Wang B, Wang S, Gong L, Zhou Z. Structural, magnetic and photocatalytic properties of Sr²⁺-doped BiFeO₃ nanoparticles based on an ultrasonic irradiation assisted self-combustion method. *Ceram Int*. 2012;38(8):6643-9. doi: 10.1016/j.ceramint.2012.05.051.
- Abdulkadir I, Jonnalagadda SB, Martincigh BS. Synthesis and effect of annealing temperature on the structural, magnetic and photocatalytic properties of (La_{0.5}Bi_{0.2}Ba_{0.2}Mn_{0.1})FeO₃-. *Mater Chem Phys*. 2016;178:196-203. doi: 10.1016/j.matchemphys.2016.05.007.
- Silva GRO, Santos JC, Martinelli DM, Pedrosa AMG, de Souza MJB, Melo DMA. Synthesis and characterization of LaNi_xCo_{1-x}O₃ perovskites via complex precursor methods. *Mater Sci Appl*. 2010;1(2):39-45. doi: 10.4236/msa.2010.12008.
- Xiao X, Hu R, Liu C, Xing C, Qian C, Zuo X, et al. Facile large-scale synthesis of β-Bi₂O₃ nanospheres as a highly efficient photocatalyst for the degradation of acetaminophen under visible light irradiation. *Appl Catal B Environ*. 2013;140-141:433-43. doi: 10.1016/j.apcatb.2013.04.037.
- Yoon M, Seo M, Jeong C, Jang JH, Jeon KS. Synthesis of liposome-templated titania nanodisks: optical properties and photocatalytic activities. *Chem Mater*. 2005;17(24):6069-79. doi: 10.1021/cm0515855.
- Fan T, Chen C, Tang Z. Hydrothermal synthesis of novel BiFeO₃/BiVO₄ heterojunctions with enhanced photocatalytic activities under visible light irradiation. *RSC Adv*. 2016;6(12):9994-10000. doi: 10.1039/C5RA26500B.
- Reddy Vanga P, Mangalaraja RV, Ashok M. Structural, magnetic and photocatalytic properties of La and alkaline co-doped BiFeO₃ nanoparticles. *Mater Sci Semicond Process*. 2015;40:796-802. doi: 10.1016/j.mssp.2015.07.078.
- Soltani T, Entezari MH. Photolysis and photocatalysis of methylene blue by ferrite bismuth nanoparticles under sunlight irradiation. *J Mol Catal A Chem*. 2013;377:197-203. doi: 10.1016/j.molcata.2013.05.004.
- Zhao D, Sheng G, Chen C, Wang X. Enhanced photocatalytic degradation of methylene blue under visible irradiation on graphene@TiO₂ dyade structure. *Appl Catal B Environ*. 2012;111-112:303-8. doi: 10.1016/j.apcatb.2011.10.012.
- Darmani RS, Esmaili A, Mortezaali A, Dehghanpour S. Photocatalytic reaction and degradation of methylene blue on TiO₂ nano-sized particles. *Optik*. 2016;127(18):7143-54. doi: 10.1016/j.ijleo.2016.04.026.
- Sakar M, Balakumar S, Saravanan P, Bharathkumar S. Compliments of confinements: substitution and dimension induced magnetic origin and band-bending mediated photocatalytic enhancements in Bi_{1-x}Dy_xFeO₃ particulate and fiber nanostructures. *Nanoscale*. 2015;7(24):10667-79.

- doi: 10.1039/C5NR01079A.
31. Mohan S, Subramanian B, Bhaumik I, Gupta PK, Jaisankar SN. Nanostructured Bi(1-x)Gd(x)FeO₃ – a multiferroic photocatalyst on its sunlight driven photocatalytic activity. *RSC Adv.* 2014;4(32):16871-8. doi: 10.1039/c4ra00137k.
 32. Hu Z, Chen D, Wang S, Zhang N, Qin L, Huang Y. Facile synthesis of Sm-doped BiFeO₃ nanoparticles for enhanced visible light photocatalytic performance. *Mater Sci Eng B.* 2017;220:1-12. doi: 10.1016/j.mseb.2017.03.005.
 33. Rahmani A, Rahimzadeh H, Beirami S. Photo-Degradation of Phenol Using TiO₂/CMK-3 Photo-Catalyst Under Medium Pressure UV Lamp. *Avicenna J Environ Health Eng.* 2018;5(1):35-41. doi: 10.15171/ajehe.2018.05.